Cytotoxic and Anti-inflammatory Cembranoids from the Soft Coral Lobophytum crassum

5 AUTHORS, INCLUDING:

Zhi-Hong Wen

National Sun Yat-sen University

205 PUBLICATIONS **2,720** CITATIONS

Yang-Chang Wu

China Medical University (ROC)

482 PUBLICATIONS **7,487** CITATIONS

Jyh-Horng Sheu

National Sun Yat-sen University

268 PUBLICATIONS **3,890** CITATIONS

Cytotoxic and Anti-inflammatory Cembranoids from the Soft Coral *Lobophytum crassum*

Chih-Hua Chao,[†] Zhi-Hong Wen,[†] Yang-Chang Wu,[‡] Hsiao-Chien Yeh,[§] and Jyh-Horng Sheu*,[†,⊥]

Department of Marine Biotechnology and Resources, National Sun Yat-sen University, Kaohsiung 804, Taiwan, Republic of China, Graduate Institute of Natural Products, Kaohsiung Medical University, Kaohsiung 807, Taiwan, Republic of China, Department of Planning and Research, National Museum of Marine Biology and Aquarium, Pingtung, 944, Taiwan, Republic of China, and Asia-Pacific Ocean Research Center, National Sun Yat-sen University, Kaohsiung 804, Taiwan, Republic of China
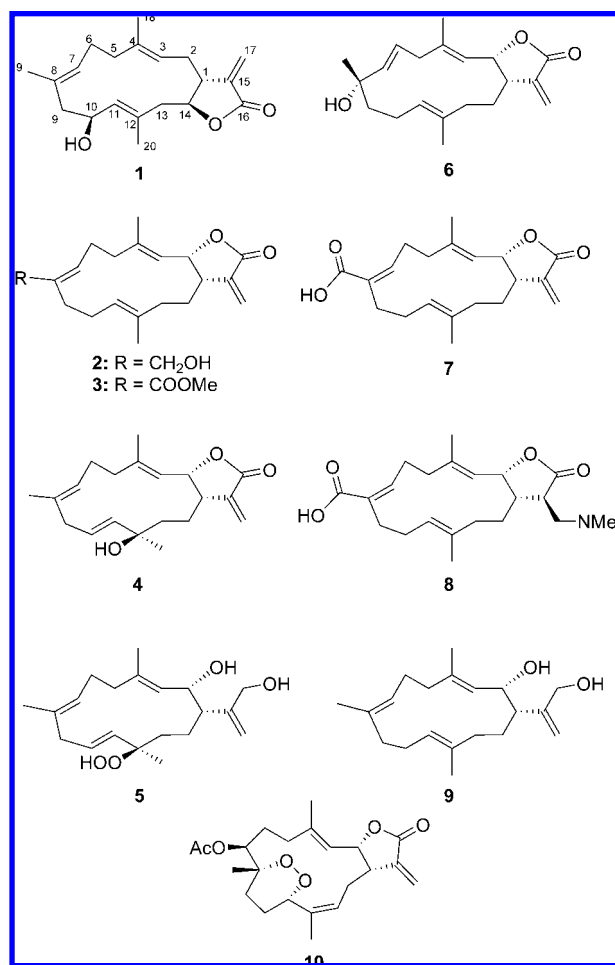
Five new cembranoids, namely, crassumolides A and B and D−F (**1** and **2** and **4**−**6**), along with four known metabolites, **7**−**10**, were isolated from the soft coral *Lobophytum crassum*. Crassumolide C (**3**) was isolated for the first time from a natural source. The structures of these compounds were elucidated by extensive spectroscopic analysis and comparison of the NMR data with those of known analogues. The absolute stereochemistry of **1** was determined using the modified Mosher's method. Chemical transformation of **7** into the corresponding methyl ester **3** revealed the absolute stereochemistry of **3**. Compounds **1**, **3**, and **7** were cytotoxic toward Ca9-22 cancer cells, and **10** was broadly cytotoxic toward all six test cancer cell lines used. Compounds **1**, **3**, **7**, and **10** were found to inhibit the accumulation of the pro-inflammatory proteins iNOS and COX-2 at 10 μM.

Soft corals of the genus *Lobophytum* have been proven to be a rich source of cembranoids and steroids, of which some have been reported to possess HIV-inhibitory,[1] cytotoxic,[2−5] and anti-inflam-matory activities.[6] A previous report has revealed that lobohedle-olide, a cembranoid isolated also from the genus *Lobophytum*,[6] possesses potent anti-inflammatory activity in a rat model. This study prompted us to investigate the bioactive metabolites of the Formosan soft coral *Lobophytum crassum* and has led to the isolation of five new cembranoids, namely, crassumolides A and B and D−F (**1** and **2** and **4**−**6**), along with four known compounds, **7**−**10**. In addition, crassumolide C (**3**) has been prepared from lobohedleolide (**7**)[7] and was isolated for the first time from a natural source in the present study. The structures of these compounds have been established by extensive spectroscopic analysis. The absolute configurations of **1** and **3** were determined by the application of the modified Mosher's method and chemical transformation of **7** into its methyl ester **3**, respectively. The cytotoxicity of compounds **1**−**10** against human liver carcinoma (HepG2 and HepG3), human breast carcinoma (MCF-7 and MDA-MB-231), human lung carci-noma (A-549), and human oral cancer cells (Ca9-22) was studied, and the ability of **1**−**3** and **6**−**10** to inhibit up-regulation of the pro-inflammatory iNOS (inducible nitric oxide synthase) and COX-2 (cyclooxygenase-2) proteins in LPS (lipopolysaccharide)-stimulated RAW264.7 macrophage cells was also evaluated.

Results and Discussion

HRESIMS of crassumolide A (**1**) exhibited a pseudomolecular ion peak at *m/z* 339.1935 [M + Na]+, consistent with the molecular formula $C_{20}H_{28}O_3$, and seven degrees of unsaturation. The IR spectrum of **1** revealed the presence of a hydroxy group (ν_{max} 3416 cm−1). The ^{13}C NMR spectrum of **1** (Table 1) displayed 20 carbon signals, and a DEPT experiment confirmed the presence of three methyls, six methylenes, six methines, and five quaternary carbons. The characteristic NMR signals at δ_C 170.2 (qC), 139.1 (qC), 123.3 (CH₂), 80.9 (CH), and 45.3 (CH) and δ_H 6.31, 5.71 (each, 1H, br s), 4.27 (1H, br d, *J* = 9.2 Hz), and 2.63 (1H, br d, *J* = 8.6 Hz) (Tables 1 and 2), in addition to the IR absorption band at 1764

* To whom correspondence should be addressed. Tel: 886-7-5252000, ext. 5030. Fax: 886-7-5255020. E-mail: sheu@mail.nsysu.edu.tw.
[†] Department of Marine Biotechnology and Resources, National Sun Yat-sen University.
[‡] Kaohsiung Medical University.
[§] National Museum of Marine Biology and Aquarium.
[⊥] Asia-Pacific Ocean Research Center, National Sun Yat-sen University.

cm−1, revealed the presence of an α-methylene-γ-lactone by comparing with data of similar metabolites.[1−4,8] Three trisubstituted double bonds were also identified from the NMR signals at δ_C 136.7 (qC), 133.2 (qC), 131.1 (qC), 131.8 (CH), 125.9 (CH), and 120.8 (CH) and at δ_H 4.91 (1H, br t, *J* = 5.0 Hz), 5.00 (1H, br t, *J* = 7.0 Hz), and 5.16 (1H, d, *J* = 9.0 Hz). The three 3H singlets appearing in the ^{1}H NMR spectrum at δ 1.74, 1.67, and 1.62 were assigned as three olefinic methyls. The above functionalities accounted for six of the seven degrees of unsaturation; the remaining degree of

Table 1. ^{13}C NMR Spectroscopic Data for Compounds **1−6**

position	**1**^{a}	**2**^{a}	**3**^{a}	**4**^{b}	**5**^{b}	**6**^{b}
1	45.3 (CH)^c	43.4 (CH)	43.1 (CH)	43.9 (CH)	50.2 (CH)	42.8 (CH)
2	29.8 (CH$_2$)	78.1 (CH)	78.0 (CH)	78.1 (CH)	71.4 (CH)	77.6 (CH)
3	120.8 (CH)	120.6 (CH)	120.5 (CH)	121.2 (CH)	127.3 (CH)	120.1 (CH)
4	136.7 (qC)	141.9 (qC)	142.2 (qC)	141.2 (qC)	136.7 (qC)	141.5 (qC)
5	38.5 (CH$_2$)	39.8 (CH$_2$)	39.9 (CH$_2$)	39.3 (CH$_2$)	39.4 (CH$_2$)	42.8 (CH$_2$)
6	24.6 (CH$_2$)	24.1 (CH$_2$)	26.4 (CH$_2$)	23.8 (CH$_2$)	24.2 (CH$_2$)	124.0 (CH)
7	125.9 (CH)	129.8 (CH)	144.9 (CH)	122.3 (CH)	122.7 (CH)	140.8 (CH)
8	131.1 (qC)	137.0 (qC)	129.8 (qC)	135.3 (qC)	134.6 (qC)	72.7 (qC)
9	46.7 (CH$_2$)	35.7 (CH$_2$)	35.4 (CH$_2$)	40.5 (CH$_2$)	41.4 (CH$_2$)	42.3 (CH$_2$)
10	66.7 (CH)	24.0 (CH$_2$)	25.0 (CH$_2$)	126.8 (CH)	129.2 (CH)	23.6 (CH$_2$)
11	131.8 (CH)	123.9 (CH)	123.1 (CH)	137.9 (CH)	133.6 (CH)	125.3 (CH)
12	133.2 (qC)	134.1 (qC)	135.1 (qC)	73.4 (qC)	85.2 (qC)	133.1 (qC)
13	47.0 (CH$_2$)	36.3 (CH$_2$)	36.2 (CH$_2$)	39.7 (CH$_2$)	39.7 (CH$_2$)	36.5 (CH$_2$)
14	80.9 (CH)	27.1 (CH$_2$)	27.0 (CH$_2$)	25.2 (CH$_2$)	21.8 (CH$_2$)	27.3 (CH$_2$)
15	139.1 (qC)	139.0 (qC)	138.9 (qC)	139.4 (qC)	147.7 (qC)	138.6 (qC)
16	170.2 (qC)	170.8 (qC)	170.7 (qC)	170.6 (qC)	66.3 (CH$_2$)	170.8 (qC)
17	123.3 (CH$_2$)	120.7 (CH$_2$)	120.7 (CH$_2$)	121.6 (CH$_2$)	115.6 (CH$_2$)	121.1 (CH$_2$)
18	16.2 (CH$_3$)	15.3 (CH$_3$)	15.3 (CH$_3$)	15.4 (CH$_3$)	15.7 (CH$_3$)	16.6 (CH$_3$)
19	17.9 (CH$_3$)	60.0 (CH$_2$)	168.1 (qC)	18.1 (CH$_3$)	17.9 (CH$_3$)	27.2 (CH$_2$)
20	16.9 (CH$_3$)	16.1 (CH$_3$)	16.1 (CH$_3$)	27.0 (CH$_3$)	23.0 (CH$_3$)	15.4 (CH$_3$)
OMe			51.2 (CH$_3$)			

^{a} Recorded at 75 MHz in CDCl$_3$ at 25 °C. ^{b} Recorded at 125 MHz in CDCl$_3$ at 25 °C. ^{c} Multiplicities deduced by DEPT.

Table 2. ^{1}H NMR Spectroscopic Data for Compounds **1−6**

| position	**1**^{a}	**2**^{a}	**3**^{a}	**4**^{b}	**5**^{b}	**6**^{b}
1	2.63 br d (8.6)^c	3.07 m	3.10 m	2.97 m	2.34 ddd (12.0, 3.0, 3.0)	3.09 m
2	2.20 m	5.40 dd (9.9, 7.9)	5.43 dd (10.0, 8.0)	5.26 dd (9.5, 7.5)	4.48 dd (8.0, 3.0)	5.38 dd (10.1, 8.2)
	2.18 m					
3	5.00 br t (7.0)	5.04 d (9.9)	5.04 d (10.0)	5.15 d (9.5)	5.28 d (8.0)	5.02 d (10.1)
5	2.14 m	2.33 m	2.37 m	2.28 m	2.22 m	2.75 dd (13.5, 7.0)
	2.05 m	2.18 m	2.20 m	2.10 ddd (12.0, 12.0, 3.0)	2.04 ddd (12.5, 12.5, 3.5)	2.68 dd (13.5, 6.0)
6	2.22 m	2.50 m	3.03 m	2.25 m	2.28 m	5.60 ddd (16.0, 7.0, 6.0)
	2.14 m	2.22 m	2.40 m	2.18 m	2.13 m	
7	4.91 br t (5.0)	4.97 br d (7.9)	5.58 dd (8.3, 3.3)	4.95 br t (5.5)	5.00 t (6.0)	5.55 d (16.0)
9	2.38 br d (14.2)	2.45 m	2.68 br d (12.3)	2.68 dd (16.0, 7.5)	2.71 dd (15.5, 8.5)	1.77 m
	2.16 m	1.93 m	1.93 m	2.62 dd (16.0, 7.5)	2.66 dd (15.5, 6.0)	
10	4.59 ddd (9.3, 9.0, 2.6)	2.12 m	2.13 m	5.61 ddd (15.5, 7.5, 7.5)	5.58 ddd (15.5, 8.5, 6.0)	2.31 m
						2.02 m
11	5.16 d (9.0)	4.95 t (7.3)	4.95 t (6.6)	5.43 d (15.5)	5.38 d (15.5)	5.00 t (6.0)
13	2.47 br d (13.4)	2.05 m	2.08 m	1.68 m	1.76 ddd (12.5, 12.5, 5.0)	2.00 m
	2.09 m	1.73 m	1.74 m	1.46 ddd (12.5, 12.5, 2.5)	1.23 ddd (12.0, 12.0, 4.0)	1.73 m
14	4.27 br d (9.2)	1.89 m	1.97 m	1.62 m	1.57 m	1.98 m
		1.47 m	1.45 m	1.28 m		1.34 m
16						
17	6.31 br s	6.25 d (3.0)	6.27 d (3.0)	6.24 d (2.0)	5.29 s	6.28 d (3.1)
	5.71 br s	5.53 d (3.0)	5.53 d (3.0)	5.59 d (2.0)	4.95 s	5.53 d (3.1)
18	1.62 s	1.68 s	1.73 s	1.65 s	1.64 s	1.80 s
19	1.67 s	4.20 d (11.8)		1.65 s	1.67 s	1.33 s
		4.06 d (11.8)				
20	1.74 s	1.58 s	1.52 s	1.31 s	1.37 s	1.59 s
OMe			3.74 s			
OOH					7.59 br s	

^{a} Recorded at 300 MHz in CDCl$_3$ at 25 °C. ^{b} Recorded at 500 MHz in CDCl$_3$ at 25 °C. ^{c} J values (in Hz) in parentheses.
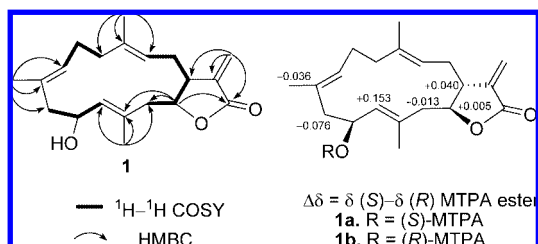
Figure 1. Selective ^{1}H−^{1}H COSY and HMBC correlations and ^{1}H NMR chemical shift differences of MTPA esters of **1**.

unsaturation was thus attributed to a 14-membered ring, as revealed by subtracting three olefinic methyls and three carbons from the γ-lactone ring. The gross structure of **1** was further established by 2D NMR studies, particularly by ^{1}H−^{1}H COSY and HMBC correlations (Figure 1). The location of a hydroxy group at C-10 [$δ_C$ 66.7 (CH); $δ_H$ 4.59 (1H, ddd, J = 9.3, 9.0, 2.6 Hz)] was deduced from the HMBC correlations from H$_3$-20 to C-11, C-12, and C-13

and the ^{1}H−^{1}H COSY correlations of H-10 with both H$_2$-9 and H-11. The planar structure of **1** was thus established.

The relative configuration of **1** was determined by the NOE correlations observed in a NOESY experiment and also with the aid of molecular modeling using MM2 force field calculations. The NOE correlations observed for H$_3$-18 with H$_2$-2 and H-7 with H-9b (δ 2.16) revealed the *E* geometry of the double bonds at C-3 and C-7. In addition, H-1 showed NOE correlations with both H-13b (δ 2.09) and H-11, while H-14 showed such responses to H-13a (δ 2.47) and H$_3$-20, suggesting the presence of a *trans*-fused γ-lactone ring in **1** (Figure 2). The same orientation of H-10 and H-14 in the molecule of **1**, in addition to the *E* geometry of the double bond at C-11, was suggested on the basis of the NOE correlations observed for H$_3$-20 with both H-10 and H-14. According to the above NOE correlations, and the others shown in Figure 2, the relative configurations at C-1, C-10, and C-14 for **1** were determined as 1R*, 10S*, and 14S*, respectively. The absolute configuration of **1** was determined by the application of Mosher's method.[9,10] The (S)- and (R)-MTPA esters of **1** (**1a** and **1b**,
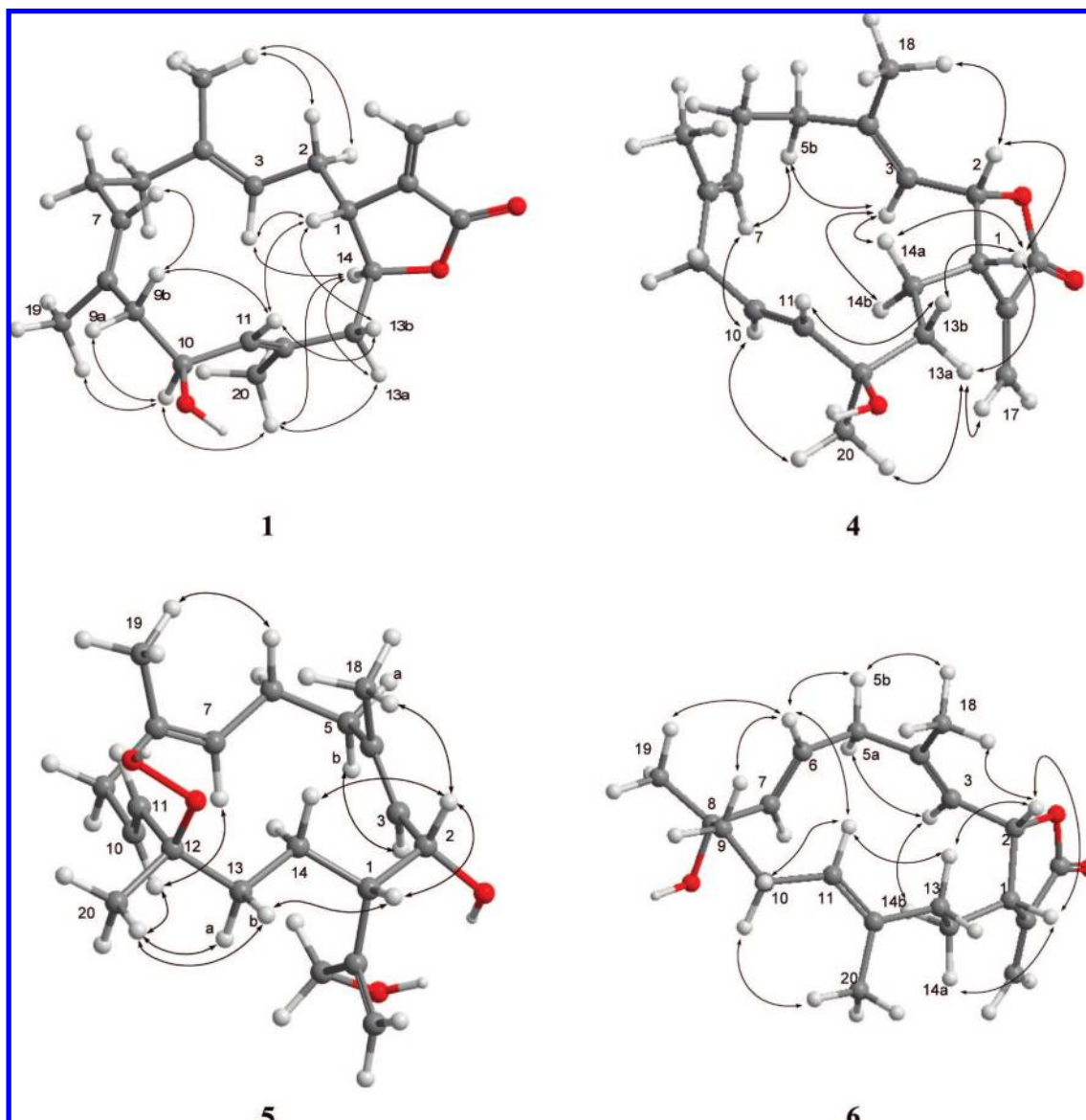
Figure 2. Key NOE correlations and computer-generated perspective model using MM2 force field calculations for **1**, **4**, **5**, and **6**.

respectively) were prepared using the corresponding (*R*)- and (*S*)-MTPA chloride, respectively. The determination of chemical shift differences for the protons neighboring C-10 led to the assignment of the *S* configuration at C-10 in **1** (Figure 1). Thus, the absolute stereochemistry of **1** was determined and was found to possess 1*R*, 10*S*, and 14*S* configurations.

HRESIMS of crassumolide B (**2**) exhibited a [M + Na]⁺ peak at *m/z* 339.1934 (calcd for $C_{20}H_{28}O_3Na$, 339.1936) and established the molecular formula $C_{20}H_{28}O_3$, implying seven degrees of unsaturation. The IR spectrum of **2** disclosed the presence of hydroxy (ν_{max} 3422 cm⁻¹) and α-methylene-γ-lactone (ν_{max} 1761 cm⁻¹) groups. The NMR spectra of **2** (Tables 1 and 2) were quite similar to those of a known compound, lobocrassolide.[2] However, resonances for the acetoxyl in lobocrassolide were absent from the NMR spectra of **2**. In addition, the acetoxyl-containing methylene protons at δ 4.55 (2H, br s) in lobocrassolide were upfield-shifted to δ 4.20 and 4.06 (each 1H, d, *J* = 11.8 Hz) in **2**. Therefore, **2** is a deacetyl derivative of lobocrassolide.

Crassumolide C (**3**) was found to possess the molecular formula $C_{21}H_{28}O_4$, as deduced from the HRESIMS and NMR spectroscopic data. The IR spectrum disclosed the presence of an α-methylene-γ-lactone (ν_{max} 1765 cm⁻¹) and an ester carbonyl (ν_{max} 1712 cm⁻¹), of which the latter was corroborated by the proton resonance at δ

3.74 (3H, s) and carbon resonances at δ 168.1 (qC) and 51.2 (CH₃). A detailed comparison of the spectroscopic data of **3** with those of lobohedleolide (**7**), a cembranoid for which the absolute stereochemistry is known, suggested that **3** might be a methyl ester of lobohedleolide.[7] However, the lack of NMR spectroscopic data for the methyl ester of **7** in the literature[7] precluded the facile structure confirmation of **3**. In order to confirm the structure, including the absolute stereochemistry of **3**, chemical conversion of **7** into the corresponding methyl ester was performed. To prevent side reactions occurring in the esterification,[7] **7** was treated with MeOH in the presence of 1-ethyl-3-(3-dimethylaminopropyl)carbodiimide hydrochloride (EDC·HCl), 4-(dimethylamino)pyridine (4-DMAP), and 4-(dimethylamino)pyridine hydrochloride (4-DMAP·HCl)[11] to obtain the corresponding methyl ester (95% yield), of which the ¹H and ¹³C NMR spectroscopic data were consistent with those of **3**. Also, the specific rotation of **3** ([α]²²_D −36) was consistent with that of the methyl ester ([α]²²_D −35) prepared from **7**, revealing that the absolute configurations at both C-1 and C-2 of **3** should be the same as those of **7**. To the best of our knowledge, **3** has been isolated for the first time from a natural source in this study.

Crassumolide D (**4**) was found to have the same molecular formula as **2** from the HRESIMS and NMR spectroscopic data. The ¹H and ¹³C NMR resonances appropriate for an α-methylene-
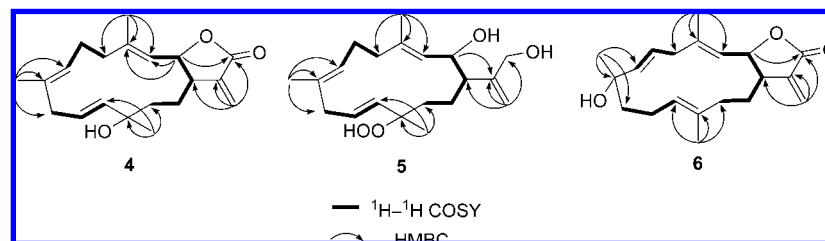
Figure 3. Selective $^1H-^1H$ COSY and HMBC correlations of **4**−**6**.

γ-lactone group were corroborated by the IR absorption at 1763 cm^{-1}. A hydroxyl-containing quaternary carbon was identified by the carbon resonance at δ 73.4 and the IR absorption at 3452 cm^{-1}. Inspection of the $^1H-^1H$ COSY spectrum of **4** led to the construction of three partial structures, as shown in Figure 3. Two methyl groups resonating at δ_H 1.65 (6H, s) were assigned as substituents of two double bonds that showed carbon resonances at δ 141.2 (qC), 135.3 (qC), 122.3 (CH), and 121.2 (CH). This was further evidenced by the HMBC correlations from H$_3$-18 (δ 1.65) to C-3, C-4, and C-5; H$_3$-19 (δ 1.65) to C-7, C-8, and C-9; and H-2 to C-3 and C-4. The 3H singlet at δ 1.31 was attributable to a methyl attached to the above-mentioned hydroxyl-containing quaternary carbon, as revealed by the HMBC correlations from this singlet to C-11, C-12, and C-13. A 15.5 Hz coupling constant between H-10 and H-11 allowed the establishment of *E* geometry of the double bond at C-10. The *E* geometry of the double bonds at C-3 and C-7 was evidenced by the presence of NOE correlations between H-3 and H-5b (δ 2.10) and between H-7 and H-10 (Figure 2). A strong NOE correlation was observed between H-1 and H-2, revealing a *cis*-fused γ-lactone ring at C-1 and C-2. In addition, H$_3$-20 showed an NOE enhancement with H-13a (δ 1.68), while H-1 correlated with H$_2$-13, suggesting that H$_3$-20 and H-1 are positioned on the opposite face of the molecule of **4**, as shown in Figure 2.

The molecular formula of crassumolide E (**5**) was found to be C$_{20}$H$_{32}$O$_4$, as deduced from the HRESIMS and NMR spectroscopic data. The IR spectrum of **5** showed the absence of a carbonyl group and the presence of a hydroxy group (ν_{max} 3290 cm^{-1}). The ^{13}C NMR and DEPT spectra of **5** (Table 1) displayed 20 carbon signals, including three methyls, seven methylenes, six methines, and four quaternary carbons. The ^1H NMR spectrum of **5** (Table 2) was similar to that of **9**,[12] except for the migration of the 11,12-double bond in **9** to a 10,11-double bond in **5** and the conversion of the olefinic quaternary carbon C-12 in **9** to an oxygenated quaternary carbon in **5**. Moreover, the hydroxy group at C-12 in **4** was found to be replaced by a hydroperoxy group in **5** from the carbon signal at δ 85.2 (qC, C-12) and the hydroperoxy proton signal at δ 7.59 (1H, br s, OOH).[13] The above interpretation and detailed inspection of the $^1H-^1H$ COSY and HMBC correlations of **5** were used to establish unambiguously its planar structure (Figure 3). In the NOESY spectrum of **5**, H-2 was found to show NOE correlations with H-1, suggesting that H-1 and H-2 were *cis*-configured. Furthermore, a 3.0 Hz coupling constant between H-1 and H-2 of **5** was found to be similar to those of cembranoids with the same 2,16-diols ($J \approx 1.5-2.2$ Hz)[12,14a] obtained from reduction of *cis*-fused γ-lactone cembranolides, rather than those of the *trans* isomers ($J \approx 9.2-10.0$ Hz).[14] Furthermore, H-1 exhibited an NOE response with H-13b, while H$_3$-20 showed a correlation with H$_2$-13 rather than H$_2$-14, revealing the opposite orientations of H-1 and H$_3$-20, as shown in Figure 2.

HRESIMS of crassumolide F (**6**) established the same molecular formula, C$_{20}$H$_{28}$O$_3$, as that of **4**, implying seven degrees of unsaturation. The ^{13}C NMR (Table 1) and IR spectroscopic data of **6** were similar to those of **4**, revealing a similar substitution pattern. The $^1H-^1H$ COSY correlations suggested three proton−proton sequences, as shown in Figure 3. The HMBC correlations from H$_3$-18 to C-3, C-4, and C-5; H$_3$-19 to C-7, C-8, and C-9; and

Table 3. Cytotoxicity Data of Compounds **1**−**10**

compound	cell lines IC$_{50}$ (μg/mL)					
	Hep G2	Hep 3B	MDA-MB-231	MCF-7	A549	Ca9-22
1	>5.0	>5.0	>5.0	>5.0	>5.0	3.2
3	>5.0	>5.0	>5.0	>5.0	>5.0	1.7
7	>5.0	4.7	>5.0	>5.0	4.6	2.8
10	2.4	2.5	2.0	2.0	2.3	1.2
doxorubicin	0.2	0.2	0.2	0.2	0.2	0.1

^{a} A compound is considered inactive with IC$_{50}$ > 5 μg/mL. ^{b} Compounds **2**, **4**−**6**, **8**, and **9** were inactive for all cell lines.

H$_3$-20 to C-11, C-12, and C-13 (Figure 2) helped establish the planar structure of **6**. NOE correlations between H-1 and H-2, H-3 and H-5a (δ 2.75), and H$_3$-20 and H-10 suggested the presence of a *cis*-fused γ-lactone ring and *E* geometry of the two double bonds at C-3 and C-11 (Figure 2). The coupling constant of 16.0 Hz between H-6 and H-7 also allowed the establishment of *E* geometry of the 6,7-double bond. In addition, H$_3$-19 was found to show an NOE interaction with H-6, which in turn interacted with H-5b (δ 2.68), while H$_3$-18 was found to show NOE responses with both H-2 and H-5b, suggesting the same orientation of H-2, H-5b, and H$_3$-19. Thus, the configuration was deduced as shown in formula **6**.

The cytotoxicity of compounds **1**−**10** against HepG2, Hep3B, MDA-MB-231, MCF-7, A-549, and Ca9-22 cancer cells is shown in Table 3. The data revealed that compounds **1**, **3**, and **7** were cytotoxic toward Ca9-22 cancer cells. Comparison of the cytotoxicity of the structurally related compounds **2**, **3**, and **7** showed that the methyl ester **3** exhibited a similar cytotoxicity profile to **7**, whereas **2**, the hydrogenated derivative of **7**, was of significantly reduced cytotoxicity relative to **7**. The known metabolite **10** showed broad cytotoxicity toward the above six cancer cell lines, with IC$_{50}$ values ranging from 1.2 to 2.5 μg/mL. We also investigated the inhibition of these compounds toward LPS-induced pro-inflammatory protein (iNOS and COX-2) expression in RAW264.7 macrophage cells by Western blot analysis (Figure 4). Compounds **1**, **3**, **7**, and **10** at a concentration of 10 μM reduced the levels of iNOS to 26.8 ± 4.5%, 2.3 ± 2.2%, 21.5 ± 7.8%, and 10.2 ± 3.8%, respectively, and COX-2 to 50.2 ± 3.2%, 34.5 ± 8.9%, 39.2 ± 9.3%, and 34.3 ± 7.5%, respectively, in comparison with those of control cells stimulated with LPS only (100% for both iNOS and COX-2). However, a decrease of β-actin (64.2 ± 8.4% relative to the control group) occurred at 10 μM of compound **3**, revealing that it may exhibit cytotoxicity against the tested macrophage cells.

Experimental Section

General Experimental Procedures. Optical rotations were measured on a JASCO P-1020 polarimeter. IR spectra were recorded on JASCO FT/IR-4100 Fourier transform infrared spectrophotometer. The NMR spectra were recorded on a Bruker AVANCE 300 FT-NMR (or Varian Unity INOVA 500 FT-NMR) instrument at 300 MHz (or 500 MHz) for ^1H (referenced to TMS, δ_H 0.0 ppm) and 75 MHz (or 125 MHz) for ^{13}C in CDCl$_3$ (referenced to the center line of CDCl$_3$, δ_C 77.0 ppm). LRMS and HRMS were obtained by ESI on a Bruker APEX II mass spectrometer. Silica gel 60 (Merck, 230−400 mesh) was used for column chromatography. Precoated silica gel plates (Merck Kieselgel 60 F$_{254}$ 0.2 mm) were used for analytical TLC. High-performance liquid
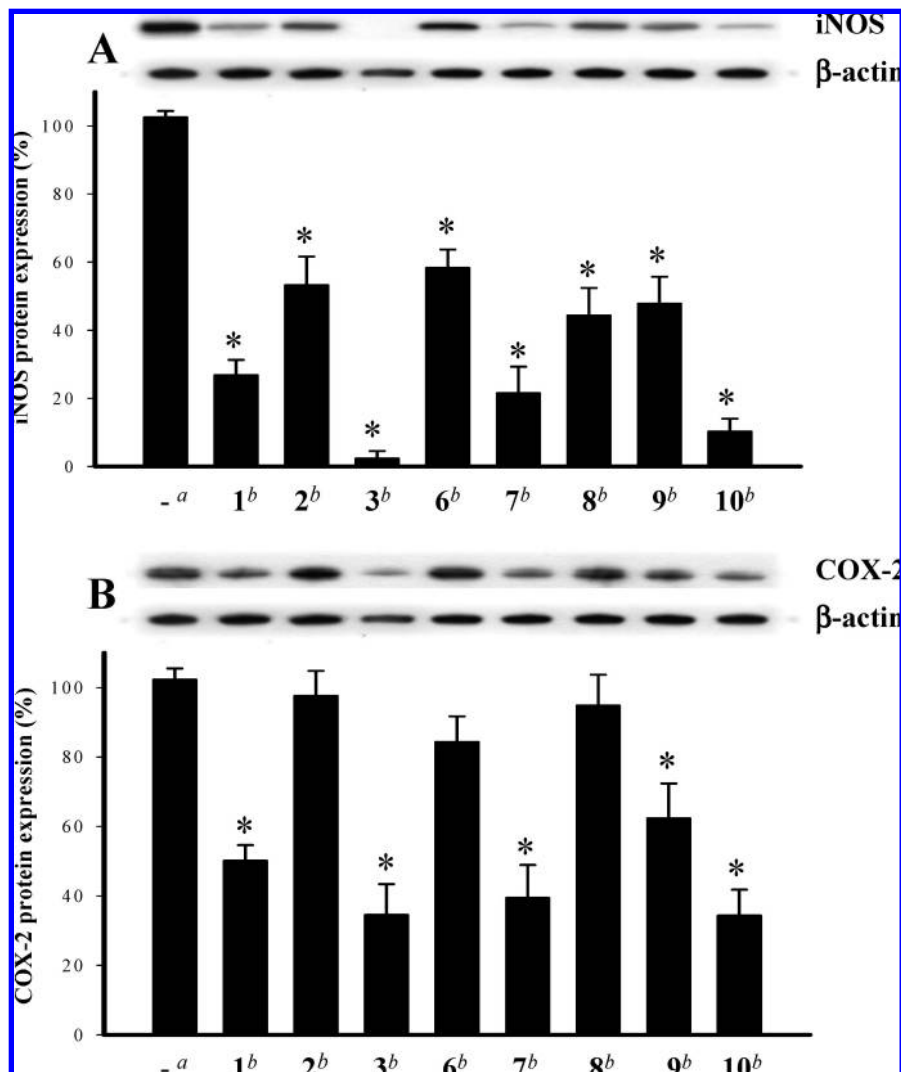
Figure 4. Effect of compounds **1**−**3** and **6**−**10** on iNOS and COX-2 protein expression of RAW264.7 macrophage cells by immunoblot analysis. (A) Immunoblots of iNOS and β-actin. (B) Immunoblots of COX-2 and β-actin. The values are means $\pm$ SEM ($n = 6$). The relative intensity of the LPS alone stimulated group was taken as 100%. Under the same experimental conditions, CAPE (caffeic acid phenylethyl ester, 10 μM) reduced the levels of the iNOS and COX-2 to 2.5 $\pm$ 3.7% and 67.2 $\pm$ 13.4%, respectively. *Significantly different from LPS alone stimulated group (*P < 0.05). [a]Stimulated with LPS. [b]Stimulated with LPS in the presence of **1**−**3** and **6**−**10** (10 μM).

chromatography (HPLC) was performed on a Shimadzu LC-10AT apparatus equipped with a Shimadzu SPD-10A UV detector. A Varian Dynamax Si-60 column (normal-phase, 250 × 21.4 mm, 100 Å, 5 μm) was used. S-(+)-α-Methoxy-α-(trifluoromethyl)phenylacetyl chloride, R-(−)-α-methoxy-α-(trifluoromethyl)phenylacetyl chloride, and 1-ethyl-3-(3-dimethylaminopropyl) carbodiimide hydrochloride (EDC·HCl) were purchased from Aldrich, and 4-(dimethylamino)pyridine (4-DMAP) was purchased from Lancaster. 4-DMAP·HCl was prepared by 4-DMAP and concentrated HCl in THF.[11]

Animal Material. The soft coral *L. crassum* was collected by hand using scuba off the coast of Kenting, in January 2004, at a depth of 10 m, and was stored in a freezer until being extracted. A voucher specimen was deposited in the Department of Marine Biotechnology and Resources, National Sun Yat-sen University (specimen no. 200401-9).

Extraction and Isolation. The soft coral *L. crassum* (1.1 kg fresh wt) was collected and freeze-dried. The freeze-dried material was minced and extracted exhaustively with EtOH (3 × 2 L). The organic extract was concentrated to an aqueous suspension and was further partitioned between EtOAc and water. The EtOAc extract (23 g) was fractionated by open column chromatography on silica gel using n-hexane−EtOAc and EtOAc−MeOH mixtures of increasing polarity to yield 19 fractions. Fraction 6, eluted with n-hexane−EtOAc (3:1), was further separated by silica gel column chromatography with gradient elution (n-hexane−acetone, 4:1 to 1:1) and followed by normal-phase HPLC (n-hexane−acetone−MeOH, 87:12:1) to yield **2** (6.3 mg), **3** (6.0

mg), **6** (4.1 mg), **9** (8.0 mg), and **10** (9.0 mg). Compound **7** (1.2 g), the major component, was obtained from fraction 7, eluted with n-hexane−EtOAc (2:1), by repeated recrystallization from n-hexane−CH$_2$Cl$_2$ (1:4). After the removal of **7**, the residue of the mother liquor of fraction 7 was fractionated by silica gel column chromatography with gradient elution (n-hexane−acetone, 4:1 to 1:1) to obtain subfractions 7A and 7B. Subfraction 7A was subjected to normal-phase HPLC (n-hexane−acetone−MeOH, 87:12:1) to afford **1** (9.7 mg). Compound **4** (1.8 mg) and an additional 100 mg of **7** were obtained from subfraction 7B by normal-phase HPLC (n-hexane−acetone−MeOH, 86:13:1). Fraction 8, eluted with n-hexane−EtOAc (1:1), was chromatographed on a silica gel column and further purified by normal-phase HPLC (n-hexane−acetone, 86:14) to yield **5** (1.5 mg). Compound **8** (9.5 mg) was obtained from fraction 13, eluted with EtOAc−MeOH (10:1), on a Sephadex LH-20 column, using acetone as eluent.

Crassumolide A (1): colorless gum; $[\alpha]^{22}_D$ −20 (c 0.97, CHCl$_3$); IR (KBr) ν_{max} 3416, 1764, 1441, 1268, 1123 cm^{-1}; ^{13}C and ^{1}H NMR data, see Tables 1 and 2; ESIMS m/z 339 [M + Na]$^+$; HRESIMS m/z 339.1935 [M + Na]$^+$ (calcd for C$_{20}$H$_{28}$O$_3$Na, 339.1936).

Crassumolide B (2): colorless gum; $[\alpha]^{22}_D$ +20 (c 0.63, CHCl$_3$); IR (KBr) ν_{max} 3422, 1761, 1313, 1115 cm^{-1}; ^{13}C and ^{1}H NMR data, see Tables 1 and 2; ESIMS m/z 339 [M + Na]$^+$; HRESIMS m/z 339.1934 [M + Na]$^+$ (calcd for C$_{20}$H$_{28}$O$_3$Na, 339.1936).

Crassumolide C (3): colorless gum; $[\alpha]^{22}_D$ +36 (c 0.30, CHCl$_3$); IR (KBr) ν_{max} 1765, 1712, 1437, 1255, 1200, 1108 cm^{-1}; ^{13}C and ^{1}H

NMR data, see Tables 1 and 2; ESIMS *m/z* 367 [M + Na]⁺; HRESIMS *m/z* 367.1884 [M + Na]⁺ (calcd for $C_{21}H_{28}O_4Na$, 367.1885).

Crassumolide D (4): colorless gum; $[\alpha]^{22}_D$ −32 (*c* 0.18, CHCl₃); IR (KBr) ν_{max} 3452, 1763, 1457, 1267 cm⁻¹; ¹³C and ¹H NMR data, see Tables 1 and 2; ESIMS *m/z* 339 [M + Na]⁺; HRESIMS *m/z* 339.1935 [M + Na]⁺ (calcd for $C_{20}H_{28}O_3Na$, 339.1936).

Crassumolide E (5): colorless gum; $[\alpha]^{22}_D$ −10 (*c* 0.15, CHCl₃); IR (KBr) ν_{max} 3290, 1440, 1040 cm⁻¹; ¹³C and ¹H NMR data, see Tables 1 and 2; ESIMS *m/z* 359 [M + Na]⁺; HRESIMS *m/z* 359.2198 [M + Na]⁺ (calcd for $C_{20}H_{32}O_4Na$, 359.2198).

Crassumolide F (6): colorless gum; $[\alpha]^{22}_D$ −22 (*c* 0.41, CHCl₃); IR (KBr) ν_{max} 3442, 1760, 1445, 1315, 1257, 1117 cm⁻¹; ¹³C and ¹H NMR data, see Tables 1 and 2; ESIMS *m/z* 339 [M + Na]⁺; HRESIMS *m/z* 339.1934 [M + Na]⁺ (calcd for $C_{20}H_{28}O_3Na$, 339.1936).

Preparation of (*S*)-and (*R*)-MTPA Esters of 1. To a solution of **1** (1.0 mg) in pyridine (0.4 mL) was added (*R*)-MTPA chloride (25 μL), and the mixture was allowed to stand for 3 h at room temperature. The reaction was quenched by the addition of 1.0 mL of water, and the mixture was subsequently extracted with EtOAc (3 × 1.0 mL). The EtOAc-soluble layers were combined, dried over anhydrous MgSO₄, and evaporated. The residue was subjected to short silica gel column chromatography using *n*-hexane−EtOAc (8:1) to yield the (*S*)-MTPA ester, **1a** (1.1 mg). The same procedure was used to prepare the (*R*)-MTPA ester, **1b** (1.0 mg from 1.1 mg of **1**), with (*S*)-MTPA chloride. ¹H NMR (CDCl₃) of **1a**: δ 7.370−7.502 (5H, m, Ph), 6.304 (1H, d, *J* = 1.7 Hz, H-17a), 5.877 (1H, ddd, *J* = 9.6, 8.8, 4.4 Hz, H-10), 5.686 (1H, d, *J* = 1.7 Hz, H-17b), 5.174 (1H, d, *J* = 9.6 Hz, H-11), 4.953−5.002 (2H, m, H-3 and H-7), 4.267 (1H, br d, *J* = 8.6 Hz, H-14), 2.607 (1H, br d, *J* = 9.1 Hz, H-1), 2.485 (1H, br d, *J* = 12.9 Hz, H-13), 2.310 (1H, br d, *J* = 14.0 Hz, H-9a), 1.611 (3H, H₃-19). ¹H NMR (CDCl₃) of **1b**: δ 7.339−7.485 (5H, m, Ph), 6.293 (1H, d, *J* = 1.7 Hz, H-17a), 5.850 (1H, ddd, *J* = 9.6, 8.5, 4.0 Hz, H-10), 5.676 (1H, d, *J* = 1.7 Hz, H-17b), 5.021 (1H, d, *J* = 9.6 Hz, H-11), 4.892−4.974 (2H, m, H-3 and H-7), 4.262 (1H, br d, *J* = 9.2 Hz, H-14), 2.567 (1H, br d, *J* = 9.5 Hz, H-1), 2.472 (1H, br d, *J* = 13.6 Hz, H-13), 2.386 (1H, br d, *J* = 14.0 Hz, H-9a), 1.647 (3H, H₃-19).

Conversion of 7 to 3. To a stirring solution of compound **7** (15 mg, 0.0455 mmol) in CH₂Cl₂ (5 mL) was successively added DMAP (6.7 mg, 0.055 mmol), 4-DMAP·HCl (8.6 mg, 0.055 mmol), and EDC·HCl (10.5 mg, 0.055 mmol). After the mixture was stirred at 0 °C for 3 h, anhydrous MeOH (0.3 mL) was added. The mixture was then warmed to room temperature and reacted overnight. The reaction was quenched by water, and the mixture was subsequently extracted with EtOAc (5 × 6 mL). The EtOAc extract was combined and successively washed with 5% aqueous HCl, saturated aqueous NaHCO₃, and brine. The organic layer was dried over anhydrous Na₂SO₄ and concentrated to give a residue, which was chromatographed on silica gel with *n*-hexane−EtOAc (4:1) as eluent to afford the corresponding methyl ester (14.8 mg, 0.043 mmol), of which the NMR spectroscopic data and specific rotation, $[\alpha]^{22}_D$ +35 (*c* 0.40, CHCl₃), were consistent with those of **3**.

Cytotoxicity Testing. Cell lines were purchased from the American Type Culture Collection (ATCC). Cytotoxicity assays were performed using the MTT [3-(4,5-dimethylthiazole-2-yl)-2,5-diphenyltetrazolium bromide] colorimetric method.[15,16]

In Vitro Anti-inflammatory Assay. The anti-inflammatory assay was modified from Ho et al.[17] and Park et al.[18] Murine RAW 264.7 macrophages were obtained from the American Type Culture Collection (ATCC, No TIB-71) and cultured in Dulbecco's modified essential medium (DMEM) containing 10% heat-inactivated fetal bovine serum, at 37 °C in a humidified 5% CO₂−95% air incubator under standard conditions. Inflammation in macrophages was induced by incubating them for 16 h in a medium containing only LPS (0.01 μg/mL; Sigma, St. Louis, MO) without the presence of test compounds. For the anti-inflammatory activity assay, compounds **1**−**3** and **6**−**10** were added to the cells 5 min before LPS challenge, respectively. Then, cells were washed with ice-cold PBS, lysed in ice-cold lysis buffer, and then centrifuged at 20000*g* for 30 min at 4 °C. The supernatant was decanted from the pellet and retained for Western blot analysis. Protein concentrations were determined by the DC protein assay kit (Bio-Rad) modified by the method of Lowry et al.[16] Samples containing equal quantities of protein were subjected to SDS-polyacrylamide gel electrophoresis, and the separated proteins were electrophoretically transferred to polyvinylidene difluoride membranes (PVDF; Immobilon-P, Millipore, 0.45 μm pore size). The resultant PVDF membranes were incubated with blocking solution and then incubated for 180 min at room temperature with antibodies against inducible nitric oxide synthase (iNOS; 1:1000 dilution; Transduction Laboratories) and cyclooxygenase-2 (COX-2; 1:1000 dilution; Cayman Chemical) proteins. The blots were detected using ECL detection reagents (Perkin-Elmer, Western Blot Chemiluminescence Reagent Plus) according to the manufacturer instructions and finally exposed to X-ray film (Kodak X-OMAT LS, Kodak, Rochester, NY). The membranes were reprobed with a monoclonal mouse anti-β-actin antibody (1:2500, Sigma) as the loading control. For the immunoreactivity data, the intensity of each drug-treated band is expressed as the integrated optical density (IOD), calculated with respect to the average optical density of the corresponding control (treated with LPS only) band. For statistical analysis, all the data were analyzed by a one-way analysis of variance (ANOVA), followed by the Student−Newman−Keuls post hoc test for multiple comparisons. A significant difference was defined as a *P* value of <0.05.

Supporting Information Available: ¹H and ¹³C NMR spectra of **1**−**6** are available free of charge via the Internet at http://pubs.acs.org.

References and Notes

(1) Rashid, M. A.; Gustafson, K. R.; Boyd, M. R. *J. Nat. Prod.* **2000**, *63*, 531−533.
(2) Duh, C. Y.; Wang, S. K.; Huang, B. T.; Dai, C. F. *J. Nat. Prod.* **2000**, *63*, 884−885.
(3) Wang, S. K.; Duh, C. Y.; Wang, Y.; Cheng, M. C.; Soong, K.; Fang, L. S. *J. Nat. Prod.* **1992**, *55*, 1430−1435.
(4) Wang, L. T.; Wang, S. K.; Soong, K.; Duh, C. Y. *Chem. Pharm. Bull.* **2007**, *55*, 766−770.
(5) Morris, L. A.; Christie, E. M.; Jaspars, M.; van Ofwegen, L. P. *J. Nat. Prod.* **1998**, *61*, 538−541.
(6) Radhika, P.; Rao, P. R.; Archana, J.; Rao, N. K. *Biol. Pharm. Bull.* **2005**, *28*, 1311−1313.
(7) Uchio, Y.; Toyota, J.; Nozaki, H.; Nakayama, M. *Tetrahedron Lett.* **1981**, *22*, 4089−4092.
(8) Huang, H. C.; Ahmed, A. F.; Su, J. H.; Chao, C. H.; Wu, Y. C.; Chiang, M. Y.; Sheu, J. H. *J. Nat. Prod.* **2006**, *69*, 1554−1559.
(9) Ohtani, I.; Kusumi, T.; Kashman, Y.; Kakisawa, H. *J. Am. Chem. Soc.* **1991**, *113*, 4092−4096.
(10) Randazzo, A.; Bifulco, G.; Giannini, C.; Bucci, M.; Debitus, C.; Cirino, G.; Gomez-Paloma, L. *J. Am. Chem. Soc.* **2001**, *123*, 10870−10876.
(11) Boden, E. P.; Keck, G. E. *J. Org. Chem.* **1985**, *50*, 2394−2395.
(12) Kobayashi, M.; Ishizaka, T.; Miura, N.; Mitsuhashi, H. *Chem. Pharm. Bull.* **1987**, *35*, 2314−2318.
(13) Su, J. H.; Ahmed, A. F.; Sung, P. J.; Chao, C. H.; Kuo, Y. H.; Sheu, J. H. *J. Nat. Prod.* **2006**, *69*, 1134−1139.
(14) (a) Bowden, B. F.; Coll, J. C.; Engelhardt, L. M.; Meehan, G. V.; Pegg, G. G.; Tapiolas, D. M.; White, A. H.; Willis, R. H. *Aust. J. Chem.* **1986**, *39*, 123−135. (b) Kobayashi, M.; Son, B. W.; Kyogoku, Y.; Kitagawa, I. *Chem. Pharm. Bull.* **1986**, *34*, 2306−2309.
(15) Alley, M. C.; Scudiero, D. A.; Monks, A.; Hursey, M. L.; Czerwinski, M. J.; Fine, D. L.; Abbott, B. J.; Mayo, J. G.; Shoemaker, R. H.; Boyd, M. R. *Cancer Res.* **1988**, *48*, 589−601.
(16) Scudiero, D. A.; Shoemaker, R. H.; Paull, K. D.; Monks, A.; Tierney, S.; Nofziger, T. H.; Currens, M. J.; Seniff, D.; Boyd, M. R. *Cancer Res.* **1988**, *48*, 4827−4833.
(17) Ho, F.-M.; Lai, C.-C.; Huang, L.-J.; Kuo, T.-C.; Chao, C.-M.; Lin, W.-W. *Br. J. Pharmacol.* **2004**, *141*, 1037−1047.
(18) Park, E.-K.; Shin, Y.-W.; Lee, H.-U.; Kim, S.-S.; Lee, Y.-C.; Lee, B.-Y.; Kim, D.-H. *Biol. Pharm. Bull.* **2005**, *28*, 652−656.
(19) Lowry, O. H.; Rosebrough, N. J.; Farr, A. L.; Randall, R. J. *J. Biol. Chem.* **1951**, *193*, 265−275.